Metal-Substrate-Mediated Plasmon Hybridization in a Nanoparticle Dimer for Photoluminescence Linewidth Shrinking and Intensity Enhancement

Supporting Information

*Guang-Can Li,[†] Yong-Liang Zhang,[†] Jing Jiang,[‡] Yu Luo,[‡] Dang Yuan Lei[†,]**

[†]*Department of Applied Physics, The Hong Kong Polytechnic University, Hong Kong, China*

[‡]*School of Electrical & Electronic Engineering, Nanyang Technological University, Nanyang Avenue 639798, Singapore*

**Address corresponding to dylei@polyu.edu.hk*

Identification of single gold nanosphere dimers with dark-field microscopy

Gold nanosphere dimers can readily be identified with the aid of a dark-field microscope. As can be seen in Figure S1, the nanosphere monomers show clear green colors, while the nanoclusters appear as bright spots. In particular, the nanosphere dimers, whose constitution is confirmed afterwards in the SEM image, show clear red colors in the dark-field image. Based on these color differences of the nanoparticles in the dark-field image, we are able to optically distinguish the gold nanosphere dimers from the monomers and measure the optical response of the nanosphere dimers before the SEM characterization. Thus, potential modifications to the optical response of the nanoparticles by the e-beam irradiation in a conventional SEM-first manner are avoided.

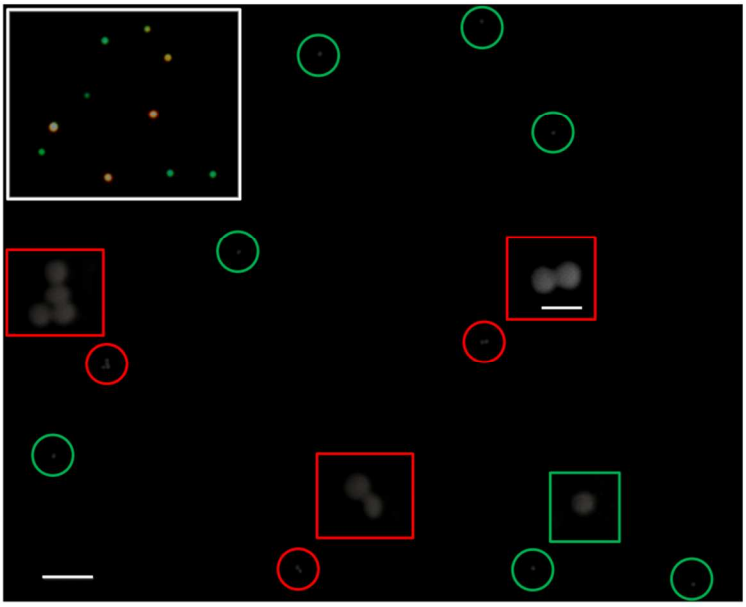

Figure S1. Pattern matched SEM image and dark-field image (inset, upper-left corner) of gold nanoparticles positioned on a 45-nm-thick gold film. The enlarged SEM image of each representative particle is presented nearby as insets. The scale bar is 1 μm in the large image and 200 nm in the enlarged image.

Simulation model of far-field radiation and photoluminescence emission for both silica- and gold-supported dimers

To simulate the far field radiation patterns of both dimer systems, the monitors used to record the radiative fields have to be very large to cover as much the radiation fields as possible and also be far enough from the surface of the gold film to avoid collecting the field of the surface waves that would not contribute to the far-field radiation. Here we adopt the finite-difference time domain (FDTD) method to calculate the far-field scattering and photoluminescence emission distribution of the two systems. As depicted in Figure S2, the lateral size of the monitors in the upper and lower half-space are set to be 4800×4800 nm^2, and symmetry planes are set in the PML boundaries to further reduce the computing burden.

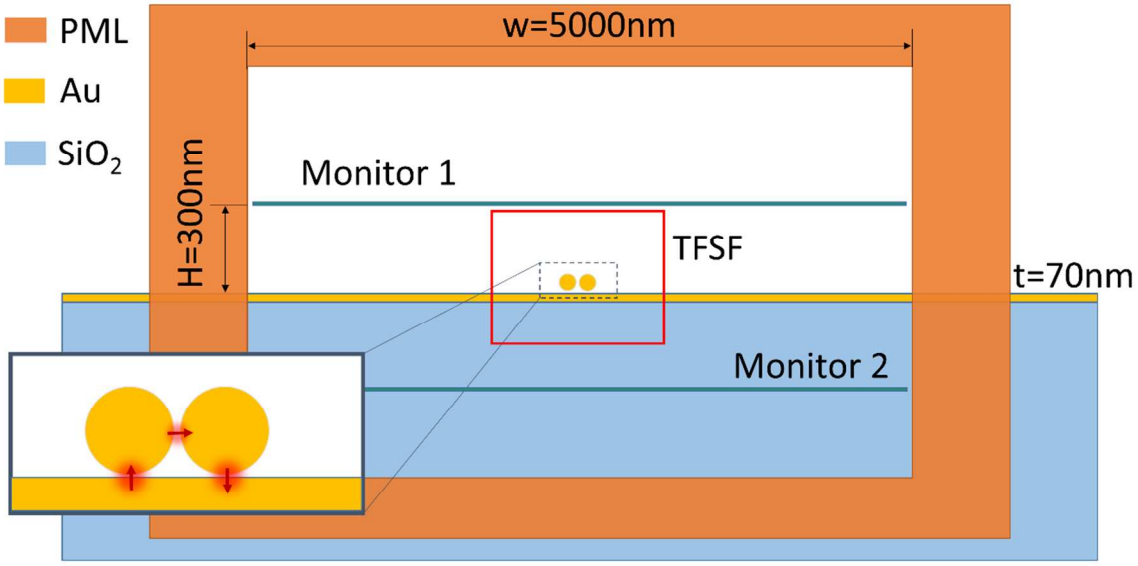

Figure S2. Schematic of an FDTD Solution (Lumerical Inc.) model for calculating the far-field radiation and photoluminescence emission patterns of the gold film-supported dimers. The same model is used for the silica-supported dimer by simply replacing the gold film layer with silica. The lateral width of the calculation domain is 5 μm. PML: perfect match layer; TFSF: total field and scattering field source. When calculating the far-field radiation pattern at the scattering peak wavelengths of the two systems, the TFSF source is launched; when calculating the photoluminescence emission patterns, the dipoles sources as shown in the inset are activated.

Scattering spectral evolution of the gold film-coupled nanosphere dimer with varying film thickness

To further understand the mechanism of the observed plasmon resonance linewidth narrowing effect, we simulate the scattering spectra of the gold film-coupled nanosphere dimer as a function of the film thickness *T* varying from 0 to 70 nm. As can be seen from Figure S3, the scattering peak shows a continuous blue shift and linewidth broadening with increasing film thickness from 0 to 25 nm, and remains unchanged for film thickness above 25 nm.

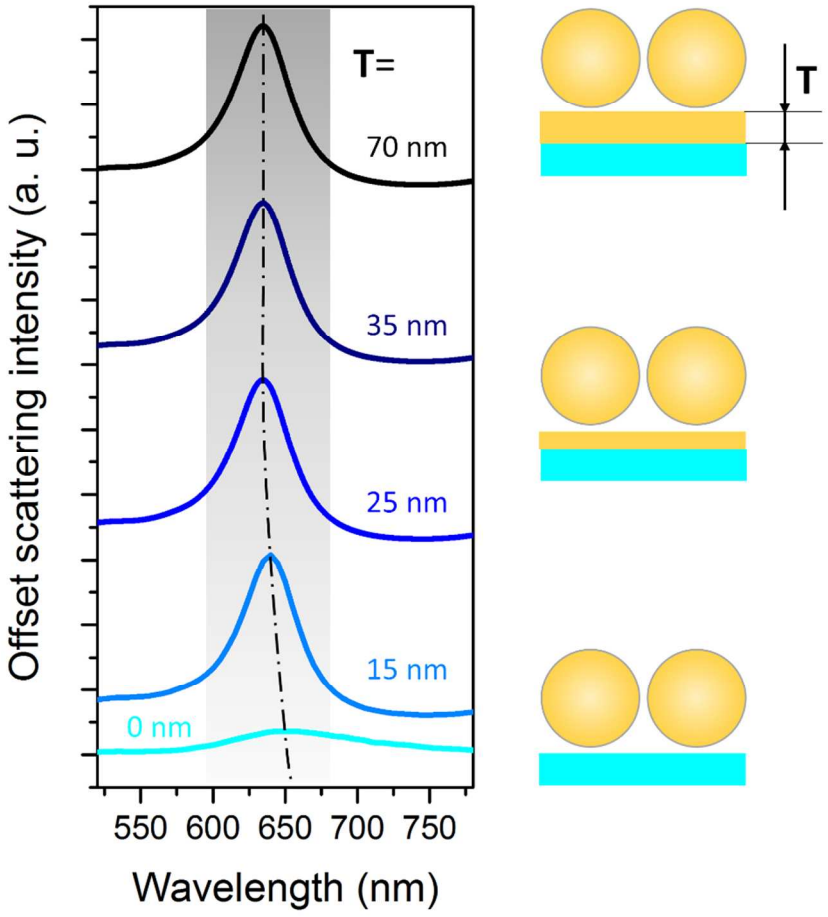

Figure S3. Simulated scattering spectra of the gold film-coupled nanosphere dimer as a function of gold film thickness. Note that the scattering spectra are offset in the y-axis for clarity. The thickness of the gold film in the simulations varies from 70 nm, 35 nm, 25 nm, 15 nm to 0 nm (corresponding to silica substrate).

Scattering spectra of a single gold film-coupled dimer taken before and after photoluminescence measurement

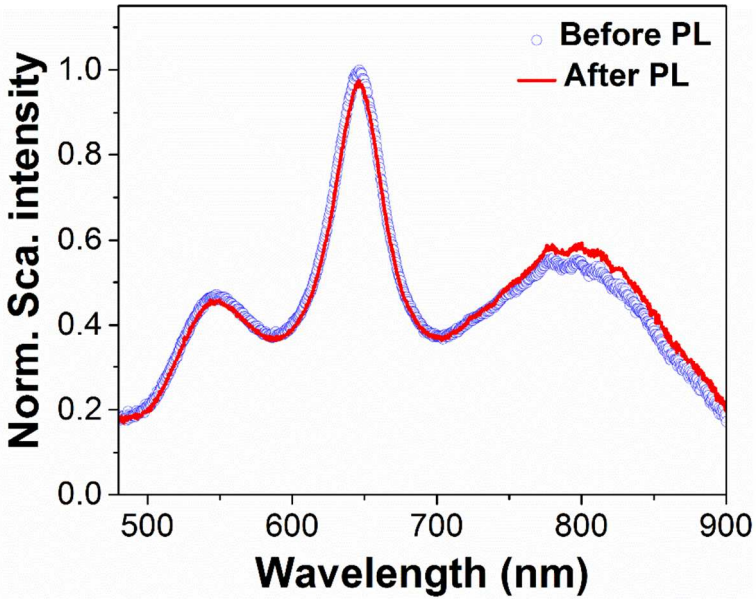

Figure S4. Scattering spectra of a single gold film-coupled gold nanosphere dimer taken before and after photoluminescence measurement. The power density of the 633nm laser is $\sim 1.6 \times 10^4$ W/cm^2 in the focus plane.

Excitation and emission polarization dependent photoluminescence spectroscopy of a silica-supported dimer under 633 nm laser illumination

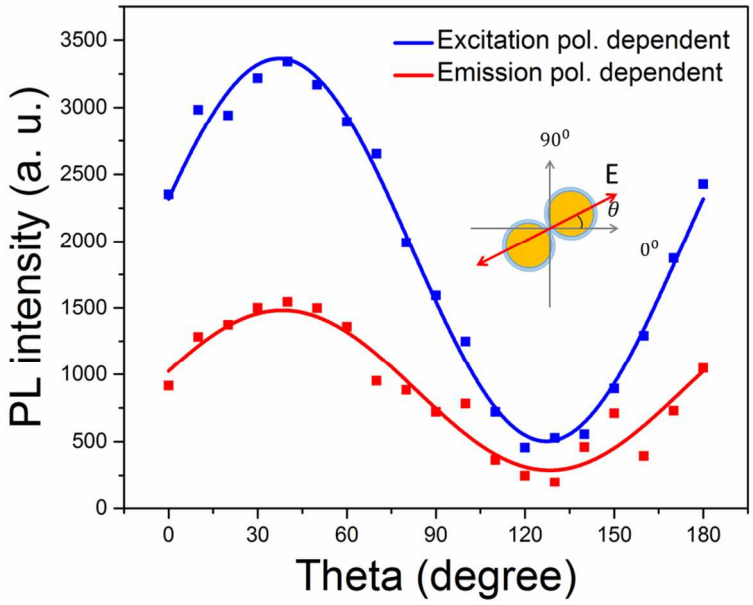

Figure S5. Excitation (blue) and emission (red) polarization dependent photoluminescence intensity under illumination by a 633 nm laser. The solid lines are fits with a cosine function: $y = A + B * cos^2(\frac{\pi}{180}x + C)$. Detailed calculations with the measured data give rise to a degree of polarization (DoP) ~0.71 for detection polarization dependence.

Comparison between photoluminescence intensities calculated over the gold film and selected slabs in a film-coupled dimer

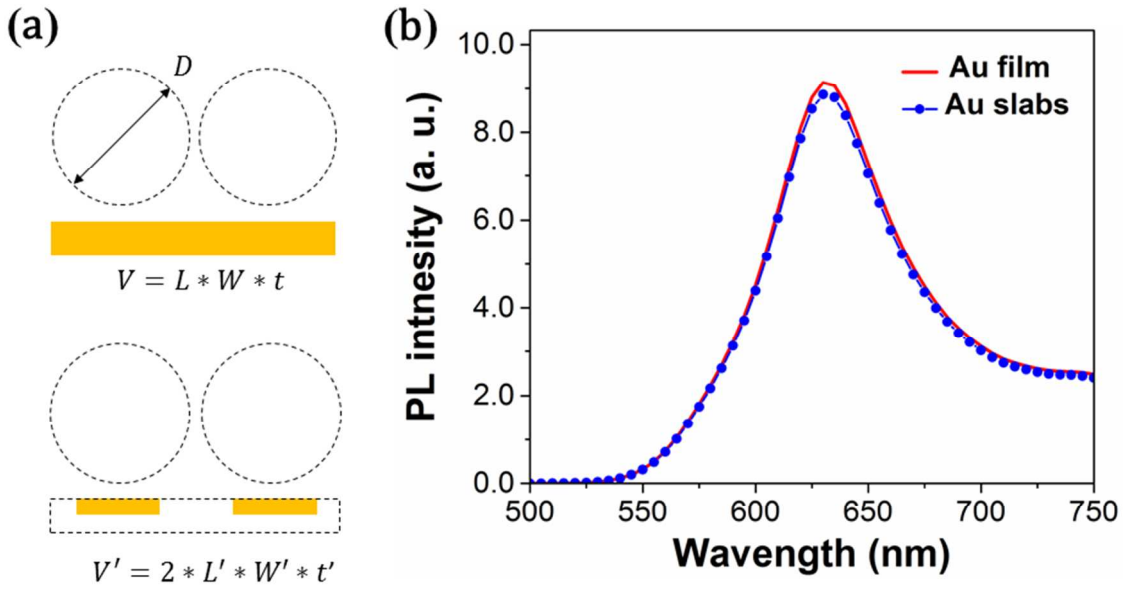

Figure S6. (a) Different integrating domains selected for calculating the photoluminescence contribution from the gold film. $L = 2D = 200$ nm, $W = 100$ nm, $t = 45$ nm, $L' = 12$ nm, $W' = 12$ nm, $t' = 6$ nm. (b) Calculated PL spectra over different domains as indicated in (a). The results confirm that the photoluminescence from the gold film is dominantly contributed by the two ultrasmall domains near the particle-film gaps. In the near-field calculations of the photoluminescence emission intensity, the override meshes applied in meshing the gold slabs, the particle-film gaps and the gold nanospheres have a mesh size of 1 nm, 0.2 nm and 1 nm, respectively. The choice of these mesh sizes as well as the mesh size for the whole simulation domain size, the number of PML layers and the conformal mesh scheme are tested to ensure the simulation convergence.

(1) Aouani, H.; Rahmani, M.; Navarro-Cía, M.; Maier, S. A. Third-Harmonic-Upconversion Enhancement from a Single Semiconductor Nanoparticle Coupled to a Plasmonic Antenna. *Nat. nanotechnol.* 2014, *9*, 290–294.

(2) Aouani, H.; Navarro-Cía, M.; Rahmani, M.; Maier, S. A. Unveiling the Origin of Third Harmonic Generation in Hybrid ITO-Plasmonic Crystals. *Adv. Opt. Mater.* 2015, *3*, 1059–1065.

(3) Viarbitskaya, S.; Teulle, A.; Marty, R.; Sharma, J.; Girard, C.; Arbouet, A.; Dujardin, E. Tailoring and Imaging the Plasmonic Local Density of States in Crystalline Nanoprisms. *Nat. mater.* 2013, *12*, 426–432.